PHYSICAL REVIEW E **75**, 015601(R) (2007)

Evidence of a mobility edge for photons in two dimensions

A. A. Asatryan, L. C. Botten, and M. A. Byrne
Centre for Ultrahigh-bandwidth Devices for Optical Systems (CUDOS) and Department of Mathematical Sciences, University of Technology, Sydney NSW 2007, Australia

R. C. McPhedran and C. M. de Sterke
CUDOS and School of Physics, University of Sydney, Sydney NSW 2006, Australia

(Received 5 October 2006; published 29 January 2007)

A scaling analysis of conductance for photons in two dimensions is carried out and, contrary to widely held belief, we find strong evidence of a mobility edge. Such behavior is compatible with the existence of an Anderson transition for electronic systems under symplectic symmetry, and indeed we show that the transfer matrix in the photonic system we have modelled has such a symmetry. We verify single parameter scaling of the conductance and demonstrate the transition from the metallic phase to localization. Key parameters, including the critical disorder, the conductance, and the critical exponent of the localization length are calculated, and it is shown that the value of the critical exponent is similar to that for electronic systems with symplectic symmetry.

DOI: 10.1103/PhysRevE.75.015601 PACS number(s): 42.25.Dd, 42.25.Fx

The phenomenological scaling theory of Anderson localization, based on the principles of renormalization [1], was the first general approach to the analysis of localization. According to this theory, all states are localized for dimensions $d \leq 2$, while for higher dimensions $d > 2$ there exists a mobility edge—the transition from diffusive propagation to localization. The derivation of this prediction assumes a system with noninteracting electrons in which the transfer matrix or Hamiltonian exhibits orthogonal symmetry. However, taking into account electron interactions it is possible to predict an Anderson transition even in two dimensions [2,3]. Other cases in which an Anderson transition is possible in two dimensions are in quantum Hall effect systems [4], in systems with symplectic symmetry in which the spin rotation symmetry is broken [5], in systems which exhibit anisotropic disorder [6,7], and even in systems in which electron interaction is weak [8]. The predictions of scaling theory in the tight binding approximation for systems with orthogonal symmetry were first tested numerically in work by Pichard *et al.* [9] and by McKinnon and Kramer [10–12]. The symplectic case of spin-orbit coupling was first considered in Refs. [13–15], and more recently in Refs. [16–19] for two-dimensional (2D) systems with a tight-binding Hamiltonian, and also for a model of a random network [20,21]. In three dimensions, the case for symplectic symmetry was considered [22], while the possibility of a mobility edge for dimensions $d < 2$ was also predicted [23]. Despite substantial research to date, there has been no corresponding treatment for photons based on a renormalization group analysis and, accordingly, in this paper we aim to address this shortcoming. We carry out our analysis using a model which provides a realistic and rigorous solution of multiple scattering, and which allows for verification by experiment. Our simulations use an exact method based on multipole field expansions, rigorously providing for all scattering orders [24]. We consider a 2D, disordered sample of Fig. 1 which we model using a supercell approach [15,21,25]. Each row of the structure is a cylinder grating, the supercell of which has period D and comprises L infinite cylinders aligned with the z axis, the centers of which are located at $x = c_j$, and periodic replicates of these. Although the cylinder positions c_j, radii a_j, and refractive indices n_j may be disordered, here we randomize only the refractive indices, taking the cylinders to be equally spaced (center-center separation $d = D/L$), of common radius a/d, and embedded in free space. The disorder is quantified by Q, with the n_j being uniformly distributed in the interval $[n-Q, n+Q]$. A slab of the photonic crystal is formed by vertically stacking L different gratings as shown in Fig. 1 and we illuminate this from above with TM ($E_{\|}$) polarized plane waves of wavelength λ, incident at some arbitrary angle.

The sample is characterized by the dimensionless conductance g—the primary parameter of scaling theory [1]—given by the generalized two-terminal Landauer formula [26,27] for multichannel propagation

$$\mathsf{g} = \sum_p \sum_q |T_{pq}|^2 = \mathrm{Tr}\, \boldsymbol{T}\boldsymbol{T}^\dagger. \tag{1}$$

Here, T_{pq} is the coefficient of transmission into plane wave channel p for unit amplitude input in channel q, with the summations taken over all propagating channels. The propagating channels in Eq. (1) are the grating orders in this case. The plane wave transmission ($\boldsymbol{T}_l$) and reflection ($\boldsymbol{R}_l$) scattering matrices for each grating layer, computed using a multi-

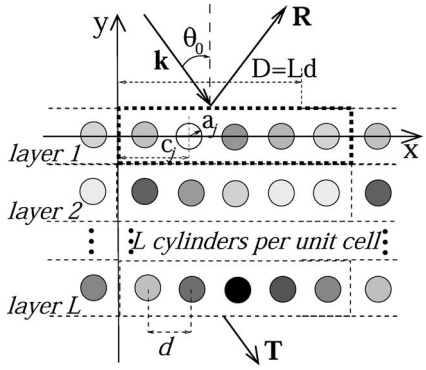

FIG. 1. Geometry of the problem for five cylinders per unit cell.

pole treatment [24], are coupled together using recurrence relations to yield the transmission and reflection matrices $(\boldsymbol{T},\boldsymbol{R})$ for the L layer slab. Since the theory includes all scattering orders, these matrices are of infinite dimension and must be truncated in computational use. Even though the calculation of g [Eq. (1)] requires only propagating states, the recursion that yields $\boldsymbol{R}$ and $\boldsymbol{T}$ requires that all propagating orders and a sufficient number of evanescent orders (N_t in total) be included to achieve a well converged solution accurately characterizing g [28].

In electronic systems, the transport properties are governed by the symmetry class of the transfer matrix $\boldsymbol{\mathcal{T}}$ (derived from $\boldsymbol{R}$ and $\boldsymbol{T}$) for the sample, and so it is natural to investigate the symmetry properties of our transfer matrix. Recently, it was established [29] using electromagnetic reciprocity arguments that, for the supercell structures we consider here, the full transfer matrix for each layer $\boldsymbol{\mathcal{T}}_l$, incorporating entries for both propagating and evanescent plane wave orders, is symplectic $\mathrm{Sp}(2N_t,\mathbb{C})$, i.e.,

$$\boldsymbol{\mathcal{T}}_l^T \boldsymbol{\mathcal{S}} \boldsymbol{\mathcal{T}}_l = \boldsymbol{\mathcal{S}}, \tag{2}$$

where $\boldsymbol{\mathcal{S}}$ has the form

$$\boldsymbol{\mathcal{S}} = \begin{bmatrix} \mathbf{0} & \boldsymbol{\sigma}_x \\ -\boldsymbol{\sigma}_x & \mathbf{0} \end{bmatrix} \quad \boldsymbol{\sigma}_x = \begin{bmatrix} \mathbf{0} & \mathbf{1} \\ \mathbf{1} & \mathbf{0} \end{bmatrix}, \tag{3}$$

and $\boldsymbol{\sigma}_x$ is the Pauli matrix of size N_t. The symplecticity is preserved by the multiplicative property of the transfer matrices and so the full transfer matrix of the slab of layers $\boldsymbol{\mathcal{T}}$ is also symplectic. The same proof establishes that the reduced form of the transfer matrix, formed by truncating $\boldsymbol{R}$ and $\boldsymbol{T}$ so they contain only propagating order channels, is also symplectic.

In our numerical simulations, we use periodic boundary conditions, with the cylinders arranged in a square $(L\times L)$ supercell array (Fig. 1), having a common radius of $a/d=0.3$, with their refractive indices distributed uniformly about $n=3$. All calculations were undertaken at the normalized wavelength $\lambda/d=2.21$. The associated regular photonic crystal has band gaps in the ranges $1.778<\lambda/d<2.137$ and $2.985<\lambda/d<3.769$. Ensemble averages of $\langle \ln \mathsf{g}\rangle$ were calculated over $N_r=4900$ realizations, with convergence studies demonstrating that each single realization of g has a relative tolerance of better than 0.017%, and with the stabilization of $\langle \ln \mathsf{g}\rangle$ with increasing N_r having been established previously [28]. To understand the effect of supercell boundary conditions, we have run our codes with both periodic and antiperiodic boundary conditions. In the localized regime, the results are almost independent of the boundary conditions, while in the diffusive regime, single realizations of $\ln \mathsf{g}$ can vary by up to 10%. The precision we achieve is sufficient for validating the single parameter scaling and establishing the existence of a mobility edge. In our analysis of the scaling theory, we follow the treatment in Slevin and Ohtsuki [30], beginning with the renormalization group equation

$$\langle \ln \mathsf{g}\rangle = F(\psi L^{1/\nu}, \phi L^{\eta}), \tag{4}$$

in which $\psi L^{1/\nu}$ is the relevant scaling function, ν is the critical exponent, and ϕ is an irrelevant scaling variable, taking into account the finite size of the sample, with $\eta<0$ required for ϕ to be regarded as irrelevant. It is possible, in general, that more than one relevant and irrelevant scaling variable is required to fit the data to Eq. (4). Here, however, we restrict ourselves to a single relevant variable (ψ), in accord with single parameter scaling theory, and a single irrelevant variable (ϕ), as justified by our results. We then approximate the scaling function (4) by a first order expansion

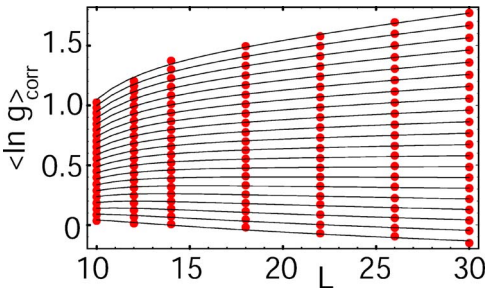

FIG. 2. (Color online) $\langle \ln \mathsf{g}\rangle$ vs L for Q ranging from $Q=0.1$ to $Q=0.3$ in steps of 0.01, from top to bottom. The dots are the actual data, while the solid lines follow from the fit (5).

$$\langle \ln \mathsf{g}\rangle = F_0(\psi L^{1/\nu}) + \phi L^{\eta} F_1(\psi L^{1/\nu}) \tag{5}$$

and expand $F_0(x)$ and $F_1(x)$ in power series

$$F_0(x) = \langle \ln \mathsf{g}\rangle_c + x + a_2 x^2 + \cdots + a_{n_0} x^{n_0}, \tag{6}$$

$$F_1(x) = 1 + b_1 x + b_2 x^2 + \cdots + b_{n_1} x^{n_1}, \tag{7}$$

where $\langle \ln \mathsf{g}\rangle_c$ is the critical value whereby, at the critical disorder $Q=Q_c$, $\langle \ln \mathsf{g}\rangle$ becomes independent of the sample size and the localization length diverges. It is then natural to write the scaling variables ψ and ϕ in series expansions of the dimensionless disorder $q=(Q_c-Q)/Q_c$:

$$\psi = \psi_1 q + \psi_2 q^2 + \cdots + \psi_{n_\psi} q^{n_\psi}, \tag{8}$$

$$\phi = \phi_0 + \phi_1 q + \phi_2 q^2 + \cdots + \phi_{n_\phi} q^{n_\phi}. \tag{9}$$

Finally, the critical exponent ν characterizes the divergence of the localization (correlation) length ξ which, when expanded about the critical point, is given by [19,30]

$$\xi = \frac{1}{|\psi_1 q + \psi_2 q^2 + \cdots + \psi_{n_\psi} q^{n_\psi}|^{\nu}}. \tag{10}$$

In Fig. 2, we show the computed values of $\langle \ln \mathsf{g}\rangle$ vs the sample size L, for $L\times L$ cells, comprising L distinct layers,

TABLE I. Estimates of the critical value parameters and confidence intervals.

P	Q_c	$\langle \ln \mathsf{g}\rangle_c$	ν
Values	0.234	0.449	2.817
95% CI	0.230–0.238	0.414–0.484	2.594–3.041
90% CI	0.231–0.238	0.419–0.478	2.630–3.004
80% CI	0.232–0.237	0.426–0.471	2.672–2.963

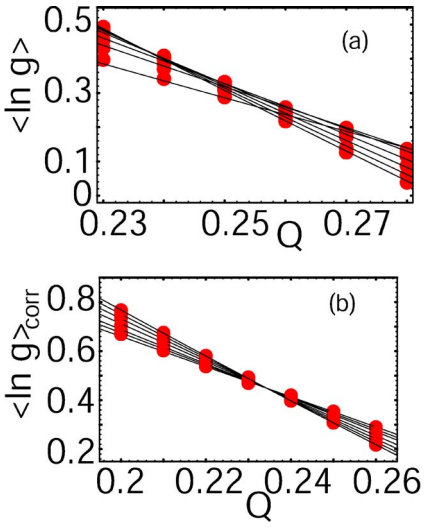

FIG. 3. (Color online) (a) $\langle \ln g \rangle$ vs Q for sizes $L=12,14,16,22,26,30$. (b) Magnified version of $\langle \ln g \rangle_{corr}$ (11) vs Q for stack sizes $L=12,14,16,22,26,30$ in the vicinity of the intersection.

each with a supercell of size L. Each curve corresponds to different disorder varying from $Q=0.1$ (top curve) to $Q=0.3$ (bottom curve) in steps of 0.01. Note that for weak disorder ($Q \leq 0.24$) the conductance increases with the system size (L), while for strong disorder ($Q>0.24$) the conductance decreases. At the critical disorder of $Q=Q_c \approx 0.24$ the conductance is independent of sample size. Such behavior is characteristic of a mobility edge in 3D electronic systems and strongly suggests the existence of a mobility edge in this 2D photonic system. We then fitted these data to the single parameter scaling model (5) using a nonlinear regression based on the Levenberg-Marquardt method [31], with the results presented in Table I and in Figs. 2–6. Note that the critical disorder does not depend on the angle of incidence since it depends on conductance, which is a summation over all incoming and outgoing channels. For a supercell of sufficient width, the calculation of the conductance samples the entire angular space of open channels and is thus independent of the incidence configuration.

In the regression, we set $n_0=3$, $n_1=1$, $n_\psi=2$, and $n_\phi=0$ and found $\eta=-4.7\pm0.7$, confirming that ϕ is indeed irrelevant. The critical exponent $\nu=2.817\pm0.223$ is close to the values calculated for symplectic 2D electronic systems using

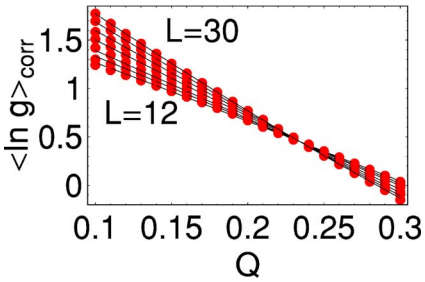

FIG. 4. (Color online) $\langle \ln g \rangle_{corr}$ vs Q for stack sizes $L=12,14,16,22,26,30$ (data corrected to compensate for finite sample size).

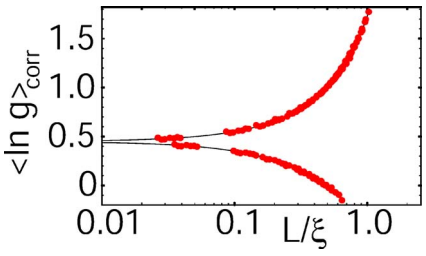

FIG. 5. (Color online) The data of Fig. 4 $\langle \ln g \rangle_{corr}$ vs L/ξ. The lower and upper branches respectively correspond to the "insulating" and "metallic" states. The dots denote data from the simulation, while the solid lines are from the fit (12).

both the Ando model $\nu=2.75\pm0.10$ [15] and a random network model $\nu=2.88\pm0.15$ [21], both of which were calculated using a supercell method with periodic boundary conditions. Plotting $\langle \ln g \rangle$ vs Q for different L (using the data of Fig. 2) we should see a common intersection point at the critical disorder Q_c. However, because of the finite size of the sample, the curves in Fig. 3(a) do not exhibit a common intersection. We rectify this by applying the ϕ scaling parameter as a correction [30],

$$\langle \ln g \rangle_{corr} = \langle \ln g \rangle - \phi L^{\eta} F_1(\psi L^{1/\nu}), \tag{11}$$

plotting the corrected data (11) in Figs. 4 and 3(b), revealing the expected common intersection at $Q_c \approx 0.234$. To demonstrate the single parameter scaling, we plot $\langle \ln g \rangle_{corr}$ vs L/ξ in Fig. 5. In this parametrization, the data distributes itself into two distinct series,

$$\langle \ln g \rangle_{corr} = F_0(\psi L^{1/\nu}) = F_0[(L/\xi)^{1/\nu}] \equiv F_{\pm}(L/\xi), \tag{12}$$

with the upper curve (F_+) corresponding to the metallic (conducting) regime (with $q>0$), and with the lower curve (F_-) corresponding to the localized (insulating) regime (with $q<0$). Finally, in Fig. 6 we consider the β function

$$\beta = \frac{d\langle \ln g \rangle_{corr}}{d \ln L}, \tag{13}$$

which is determined from the fit of the data in Fig. 4. Negative and positive values of β are associated with localized and delocalized states, respectively. Note that β changes sign at the critical value $\langle \ln g \rangle_c \approx 0.449$ associated with the critical disorder $Q=Q_c$. The conductance probability distribution

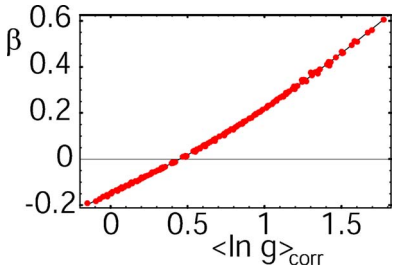

FIG. 6. (Color online) $\beta(g)$ vs $\langle \ln g \rangle_{corr}$ showing the existence of the mobility edge at $\langle \ln g \rangle_{corr} \approx 0.449$ (solid line is the fit, and dots are the data).

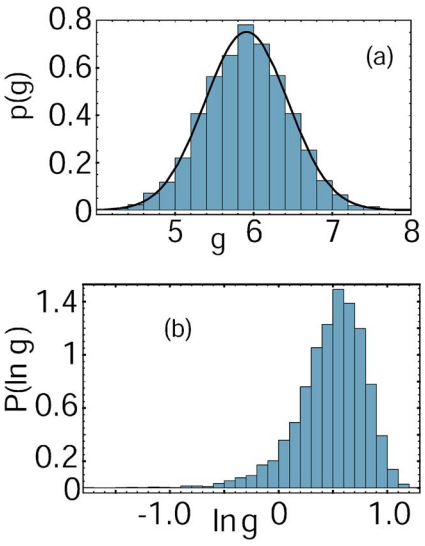

FIG. 7. (Color online) (a) Conductance probability distribution $p(\mathsf{g})$ for the metallic regime ($Q=0.1$), the solid line is the Gaussian fit calculated from the data; (b) conductance probability distribution $p(\ln \mathsf{g})$ at the transition $Q=0.23\approx Q_c$, with the typical asymmetric "tail" visible.

has also been calculated and is found to be Gaussian [see Fig. 7(a)] in the metallic regime. At the transition, the distribution $p(\ln \mathsf{g})$ exhibits the typical asymmetric behavior of Fig. 7(b), while in the localized regime, the distribution is log normal [28]. We also undertook simulations for TE ($H_{\|}$) polarization. However, the scattering is now much weaker and thus much larger systems need to be studied, requiring a concomitant increase in computational requirements.

In conclusion, we have validated single parameter scaling theory for disordered photonic systems in two dimensions using a renormalization group formalism. We have found strong numerical evidence of an Anderson transition for such systems and we explain this in terms of the symplectic nature of the system's transfer matrix, noting that mobility edges for dimension $d \leq 2$ are predicted in electronic systems with spin orbit coupling that exhibit this class of symmetry [23]. It is interesting that the value of the critical exponent we find in the electromagnetic case agrees to within error bars with those from two symplectic models of electronic systems. While the numerical evidence of an Anderson transition in two dimensions is strong, either an analytical approach or clear experimental results are needed to establish its existence unambiguously.

This work was produced with assistance from the Australian Research Council under its Discovery Grants and Centres of Excellence Programs. The provision of computing support from ac3 and APAC supercomputing centers is also acknowledged.

[1] E. Abrahams, P. W. Anderson, D. C. Licciardello, and T. V. Ramakrishnan, Phys. Rev. Lett. **42**, 673 (1979).
[2] B. Rosenstein and T. Minh-Tien, Phys. Rev. B **68**, 245321 (2003).
[3] E. Abrahams, S. V. Kravchenko, and M. P. Sarachik, Rev. Mod. Phys. **73**, 251 (2001).
[4] B. Huckestein, Rev. Mod. Phys. **67**, 357 (1995).
[5] S. Hikami, A. I. Larkin, and Y. Nagaoka, Prog. Theor. Phys. **63**, 707 (1980).
[6] Q.-J. Chu and Z.-Q. Zhang, Phys. Rev. B **48**, 10761 (1993).
[7] G. Samelsohn and V. Freilikher, Phys. Rev. E **70**, 046612 (2004).
[8] E. Ribeiro, R. D. Jäggi, T. Heinzel, K. Ensslin, G. Medeiros-Ribeiro, and P. M. Petroff, Phys. Rev. Lett. **82**, 996 (1999).
[9] J. L. Pichard and G. Sarma, J. Phys. C **14**, L127 (1981); **14**, L617 (1981).
[10] A. MacKinnon and B. Kramer, Phys. Rev. Lett. **47**, 1546 (1981).
[11] A. MacKinnon and B. Kramer, Z. Phys. B: Condens. Matter **53**, 1 (1983).
[12] B. Kramer and A. MacKinnon, Rep. Prog. Phys. **56**, 1470 (1993).
[13] S. N. Evangelou and T. Ziman, J. Phys. C **20**, L235 (1987).
[14] T. Ando, Phys. Rev. B **40**, 5325 (1989).
[15] U. Fastenrath, G. Adams, R. Bundschuh, T. Hermes, B. Raab, I. Schlosser, T. Wehner, and T. Wichmann, Physica A **172**, 302 (1992).
[16] S. N. Evangelou, Phys. Rev. Lett. **75**, 2550 (1995).
[17] K. Yakubo and M. Ono, Phys. Rev. B **58**, 9767 (1998).
[18] L. Schweitzer and I. Kh. Zharekeshev, J. Phys.: Condens. Matter **9**, L441 (1997).
[19] Y. Asada, K. Slevin, and T. Ohtsuki, Phys. Rev. Lett. **89**, 256601 (2002).
[20] R. Merkt, M. Janssen, and B. Huckestein, Phys. Rev. B **58**, 4394 (1998).
[21] K. Minakuchi, Phys. Rev. B **58**, 9627 (1998).
[22] T. Kawarabayashi, T. Ohtsuki, K. Slevin, and Y. Ono, Phys. Rev. Lett. **77**, 3593 (1996).
[23] Y. Asada, K. Slevin, and T. Ohtsuki, Phys. Rev. B **73**, 041102(R) (2006).
[24] L. C. Botten, N. A. Nicorovici, A. A. Asatryan, R. C. McPhedran, C. Martijn de Sterke, and P. A. Robinson, J. Opt. Soc. Am. A **17**, 2165 (2000); **17**, 2177 (2000).
[25] J. B. Pendry and A. MacKinnon, Phys. Rev. Lett. **69**, 2772 (1992).
[26] D. S. Fisher and P. A. Lee, Phys. Rev. B **23**, 6851 (1981).
[27] E. N. Economou and C. M. Soukoulis, Phys. Rev. Lett. **46**, 618 (1981).
[28] A. A. Asatryan, L. C. Botten, M. A. Byrne, T. N. Langtry, N. A. Nicorovici, R. C. McPhedran, C. M. de Sterke, and P. A. Robinson, Phys. Rev. E **71**, 036623 (2005).
[29] L. C. Botten, T. P. White, A. A. Asatryan, T. N. Langtry, C. Martijn de Sterke, and R. C. McPhedran, Phys. Rev. E, **70**, 056606 (2004).
[30] K. Slevin and T. Ohtsuki, Phys. Rev. Lett. **82**, 382 (1999).
[31] W. H. Press, B. P. Flannery, S. A. Teukolsky, and W. T. Vetterling, *Numerical Recipies in Fortran* (Cambridge University Press, Cambridge, England, 1992).